CNS Neuroscience & Therapeutics

ORIGINAL ARTICLE

CNS Neuroscience & Therapeutics

Astrocytic JWA Expression is Essential to Dopaminergic Neuron Survival in the Pathogenesis of Parkinson's Disease

Shu-Han Miao,[1] Hong-Bin Sun,[2] Yang Ye,[1,3] Jing-Jing Yang,[1] Yao-Wei Shi,[1] Ming Lu,[2] Gang Hu[2] & Jian-Wei Zhou[1]

1 Department of Molecular Cell Biology and Toxicology, School of Public Health,Nanjing Medical University, Nanjing, Jiangsu, China
2 Jiangsu Key Laboratory of Neurodegeneration, Department of Pharmacology, Nanjing Medical University, Nanjing, Jiangsu, China
3 Department of Preventive Medicine, School of Medical Science and Laboratory Medicine, Jiangsu University, Zhenjiang, Jiangsu, China

Keywords
Dopamine; JWA; NF-κB; Parkinson's disease; Reactive oxygen species.

Correspondence
Professor Jian-Wei Zhou, M.D., Ph.D., Department of Molecular Cell Biology and Toxicology, School of Public Health, Nanjing Medical University, 140 Hanzhong Road, Nanjing, Jiangsu 210029, China.
Tel.: +86-25-8686-8421;
Fax: +86-25-8686-8421;
E-mail: jwzhou@njmu.edu.cn
Received 21 October 2013; revision 9 February 2014; accepted 13 February 2014

doi: 10.1111/cns.12249

The first two authors contributed equally to this work.

SUMMARY

Aims: To investigate the role of astrocytic JWA expression in dopaminergic (DA) neuron degeneration and in the pathogenesis of Parkinson's disease (PD). **Methods:** Conditional astrocytic JWA null ($JWA^{\Delta 2/\Delta 2}$/GFAP-Cre) mice and U251 glioma cells were used to evaluate the effects of JWA gene on DA neuron degeneration. The oxidative stress-driven molecular events were determined in both *in vivo* and *in vitro* models. **Results:** Conditional astrocytic JWA knockout resulted in significant activation of astrocytes measured by increase in glial fibrillary acidic protein-positive cells ($1.34 \times 10^3 \pm 74.5$ vs. $8.44 \times 10^3 \pm 1.35 \times 10^3$, $P < 0.01$) in mouse substantia nigra, accompanied by loss of DA neurons ($1.03 \times 10^4 \pm 238$ vs. $6.17 \times 10^3 \pm 392$, $P < 0.001$). Deficiency of JWA significantly aggravated reactive oxygen species (ROS) accumulation in substantia nigra compared with the wild-type mice. Increasing JWA expression in U251 glioma cells inhibited ROS with a concomitant increase in intracellular glutathione. Furthermore, suppression of IKKβ-nuclear factor (NF)-κB signaling pathway was shown to regulate JWA in a PD model. **Conclusions:** The JWA gene exerts neuroprotective roles against DA neuronal degeneration via modulating intracellular redox status and NF-κB signaling pathway and is a potential treatment target for PD.

Introduction

Parkinson's disease (PD) is the second most common neurodegenerative disease characterized by muscle rigidity, tremor, postural instability and paucity of voluntary movements [1], where only symptomatic treatment currently exists [2]. The main neuropathological features of PD are the progressive degeneration of dopaminergic (DA) neurons and apparent gliosis with the presence of intracytoplasmic inclusions (Lewy bodies) in the mesencephalic substantia nigra compacta (SNc) [3,4]. Although several possible mechanisms of PD have been proposed, such as aging, oxidative stress and neuroinflammation, the explicit mechanism remains elusive [5,6]. Therefore, new strategies or drugs to reverse or ameliorate the pathological process of DA neurons in PD patients would be of great clinical value.

Oxidative damage has been considered a primary pathogenic mechanism of nigral DA neuronal cell death in PD [7]. The 1-methyl-4-phenyl-1,2,3,6-tetrahydropyridine (MPTP) neurotoxin is used in several animal models of PD as it can replica number of clinical and pathological disease hallmarks [3]. The MPTP as well as its toxic metabolite, 1-methyl-4-phenylpyridinium (MPP^+), applied extensively in *in vivo* and *in vitro* models of PD, causes degeneration of nigrostriatal DA neurons mediated by reactive oxygen species (ROS) generation and activation of cell death signaling pathways [8,9].

In the molecular and pathway level, PD has been associated with both DNA damage and abnormal activation of nuclear factor (NF)-κB, which is a known mediator of tissue damage and inflammation cellular responses [10]. The canonical activation of NF-κB is mediated by the upstream IκB kinase (IKK), a heterotrimer consisting of 2 catalytic subunits, IKKα and IKKβ, and a regulatory subunit termed IKKγ, the NF-κB essential modulator (NEMO) [11]. By exposure to various stimuli including oxidative stress, proinflammatory cytokines, and growth factors, IKK is phosphorylated, leading to IκB polyubiquitination and proteasomal degradation. Degradation of IκB induces translocation of NF-κB into the nucleus, where NF-κB binds to its cognate DNA sequences as well as its coactivators ultimately to regulate gene expression [12].

The astrocytes are star-shaped glial cells in the brain and spinal cord and the most abundant cells of the human brain. Astrocytes are multifunctional, with critical roles in biochemical support of endothelial cells that form the blood–brain barrier and a role in the repair process of the brain and spinal cord following traumatic injuries [13]. Astrocytes also play crucial roles in adult central nervous system homeostasis [14], including synaptic glutamate uptake [15], extracellular potassium maintenance [16] and nutrient support for neurons [17]. Importantly, they are critical participants in several neurodegenerative diseases, including PD [18,19].

The *JWA* gene, also known as *ARL6ip5* (ADP-ribosylation-like factor 6 interacting protein 5), codes for a novel microtubule-binding protein, which regulates cancer cell migration via MAPK cascades [20] and mediates differentiation of leukemic cells [21,22]. Moreover, it is also a key regulator in base excision repair (BER) of oxidative stress-induced DNA damage by XRCC1 stability regulation [23,24]. These findings imply that JWA is essential to maintain redox homeostasis and may also regulate inflammatory responses. However, the role of JWA gene in the pathogenesis of PD has never been investigated. In this first study, the astrocytic JWA null ($JWA^{\Delta2/\Delta2}$/GFAP-Cre) mouse model and the U251 glioma cells were used to elucidate the potential function of JWA on PD.

Materials and methods

The Institutional Animal Care and Use Committee of the Nanjing Medical University, Nanjing, China, approved the study protocol.

Preparation of Astrocytic JWA Null Mice and MPTP Administration

The exon2 of JWA was floxed with Loxp site (JWA^{L}), as described previously [25], after GFAP-Cre [26]-mediated recombination, the astrocyte exon2 was deleted ($JWA^{\Delta2}$) (Figure 1A). Intercrossing the astrocytic $JWA^{\Delta2/+}$ mice produced $JWA^{\Delta2/\Delta2}$/GFAP-Cre mice, lacking JWA in astrocytes. Genotyping of Loxp and genotyping of GFAP-Cre is shown in Figure 1B,C and Figure 1D,E, respectively. Genotyping of astrocytic JWA null mice was identified at the DNA level (Figure 1F). Post-mortem midbrain slices were stained by JWA (green), GFAP (red) and TH (red) immunofluorescence to visualize $JWA^{\Delta2/\Delta2}$/GFAP-Cre mice construction. As shown in Figure 1G, JWA (green) was expressed in GFAP-positive cells of $JWA^{Loxp/Loxp}$ (JWA colocalized with GFAP) but not found in $JWA^{\Delta2/\Delta2}$/GFAP-Cre mice. The JWA gene exhibited very low expression level (almost undetectable) in DA neurons in the basic state (Figure S1A).

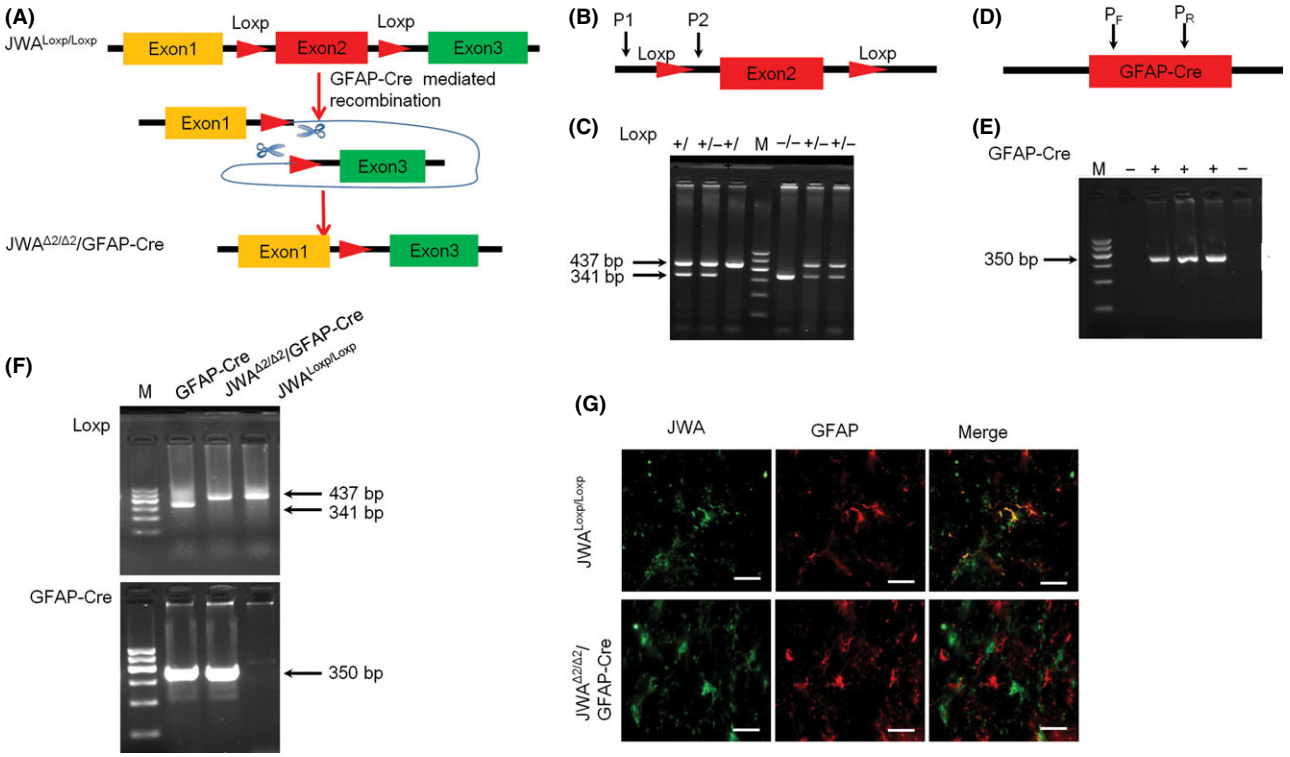

Figure 1 Construction and genotype verification of astrocytic JWA knockout mice. (**A**) The construction of $JWA^{\Delta2/\Delta2}$/GFAP-Cre. (**B**, **C**) Genotyping of Loxp mice by PCR. (**D**, **E**) Genotyping of GFAP-Cre mice by PCR. Both P_F and P_R primers were used (**D**), and the GFAP-Cre mice showed a 350 bp fragment. (**F**) Genotyping of $JWA^{\Delta2/\Delta2}$/GFAP-Cre and $JWA^{Loxp/Loxp}$ mice by PCR. The $JWA^{\Delta2/\Delta2}$/GFAP-Cre mice were identified with both 437 and 350 bp fragments; and the $JWA^{Loxp/Loxp}$ mice were identified only with 437 bp band. (**G**) The immunofluorescence staining of JWA and GFAP expression in mice midbrain. ×200 magnification. Scale bars = 40 μm.

The homozygous astrocytic JWA knockout (KO) mice ($JWA^{\Delta 2/\Delta 2}$/GFAP-Cre) were obtained for MPTP treatment. Adult male C57BL/6J mice (12–16 weeks, 26–32 g) with astrocytic JWA KO ($JWA^{\Delta 2/\Delta 2}$/GFAP-Cre) and littermate wild-type controls (WT, $JWA^{Loxp/Loxp}$) were housed in a specific pathogen-free (SPF) environment (ambient temperature, 22.0 ± 1.0°C; humidity, 40%) and provided with standard rodent chow and water.

The WT and KO mice were divided into two groups each, vehicle or MPTP treatment, four mice in each group. The chronic MPTP intoxication protocol was as described previously; briefly, 20 mg/kg MPTP (Sigma Chemicals, St. Louis, MO, USA) in saline was injected subcutaneously, and 250 mg/kg probenecid (Sigma Chemicals) in DMSO was injected intraperitoneally 1 h later, every 3.5 day over a period of 5 weeks. Mice in the vehicle group were treated similarly with saline alone.

Immunohistochemical Studies and Quantitative Evaluation

These experiments were carried out according to our standard protocols for single- or double-labeled immunostaining [27]. Primary antibodies were monoclonal mouse anti-TH (1:1000; Sigma, St. Louis, MO, USA), monoclonal mouse anti-GFAP (1:1000; Millipore, Temecula, CA, USA), and monoclonal mouse anti-JWA (1:200; contract produced by AbMax, Beijing, China). Images were captured with confocal laser scanning microscope (Axiovert LSM510; Carl Zeiss Co., Jena, Germany). The total numbers of GFAP-immunoreactive (IR) neurons and TH-IR neurons in entire extent of substantia nigra pars compacta from all four samples per group were counted. As described previously [28,29], the total numbers of GFAP and TH-positive cells were provided through Stereo-Investigator software (MicroBright Field. Inc., Williston, VT, USA).

Immunofluorescence Analysis

Immunofluorescence was carried out on the frozen brain sections. The experiments were performed according to the standard protocols [30,31]. The primary antibodies were monoclonal mouse anti-γ-aminobutyric acid (GABA, 1:100; Sigma) and polyclonal rabbit antidopamine beta hydroxylase (DBH, 1:1000; Abcam, Cambridge, UK). The second antibodies were Alexa Fluor 488-labeled goat anti-rabbit IgG (1:1000; Beyotime, Jiangsu, China) and Alexa Fluor 488-labeled goat anti-mouse IgG (1:1000; Beyotime). The frozen brain sections were mounted on Vectashield (Vector Laboratories, Peterborough, UK), which contained 1.5 μg/mL DAPI.

High-performance Liquid Chromatography

Under chloral hydrate anesthesia (400 mg/kg, i.p.), six mice striatum tissues in each group were prepared for measurement of DA, dihydroxyphenylacetic acid (DOPAC), and homovanillic acid (HVA) contents with HPLC/ECD analysis. HPLC/ECD system (Thermo, Shandon, Pittsburgh, PA, USA) consisted of a pump, an autosampler, a solvent delivery system and a Coulochem III detector equipped with a Model 5300 CouloChem III, a Model 5041 analytical cell and a Model 5020 guard cell. The mobile phase consisted of 0.075 M Na_2HPO_4, 1.7 mM OSA, 0.05 M citrate, 0.05 M EDTA, 10% methanol, and 1.0 mM 1-heptanesulfonic acid.

Cell Culture

The U251 glioma cells were purchased from Keygen (Nanjing, China). The cells were cultured in Dulbecco's modified Eagle's media (Gibco, Life Technologies, Grand Island, NY, USA) supplemented with 10% fetal bovine serum, 100 U/mL of penicillin, and 100 μg/mL of streptomycin (Gibco, Life Technologies). All the cells were maintained in 5% CO_2 atmosphere at 37°C.

Western Blotting Analysis

Under chloral hydrate anesthesia (400 mg/kg, i.p.), three mice midbrain tissues of each group were dissected on ice after sacrifice. Total cell lysates were prepared with a detergent lysis buffer for Western blotting [50 mM Tris, pH 7.4, 1% NP-40, 150 mM NaCl, 0.5% sodium deoxycholate, 0.1% SDS, 1 mM PMSF]. The nuclear extracts were aquired according to the NE-PER Nuclear and Cytoplasmic Extraction Reagents (Pierce Biotechnology, Rockford, IL, USA). Western blotting was performed as previously reported [32]. The protein in samples was extracted using the protein extraction kit (Keygen); the supernatants (50 μg protein) were separated by 12.5% Tris-glycine SDS-PAGE, transferred to PVDF membranes by the electrophoretic transfer system (Bio-Rad, Hercules, CA, USA), and blocked with 10% nonfat dry milk in Tris-HCl buffer saline, TBS, pH 7.4, containing 0.1% Tween 20 (TBST) for 1 h at room temperature. The PVDF membranes were incubated with primary monoclonal mouse antibody against JWA (1:200; contract produced by AbMax), polyclonal rabbit anti-p-p65 (1:1000; CST, USA), polyclonal rabbit anti-p65 (1:1000; Santa Cruz, CA, USA), polyclonal rabbit anti-IKKβ (1:1000; CST, USA), polyclonal rabbit IKKα (1:1000; CST, USA), polyclonal rabbit anti-IKKγ (1:1000; CST, USA), polyclonal mouse anti-IκB (1:1000; CST, USA), polyclonal mouse anti-aldolase (1:500; Santa Cruz, CA, USA), monoclonal mouse anti-FLAG (1/1000, Beyotime), polyclonal mouse antihistone H1 (1:500; Santa Cruz, CA, USA), or monoclonal mouse anti-β-actin (1/1000, Beyotime) overnight at 4°C. The membranes were incubated with corresponding secondary antibody for 1 h at room temperature after being washed in TBST. The secondary antibodies were biotinylated goat anti-mouse antibody or biotinylated goat anti-rabbit antibody (1:1000, Beyotime). We used β-actin to detect the protein-loading control, whereas histone H1 and aldolase were used for the nuclear and cytoplasmic controls, respectively.

In Situ Detection of ROS

Dihydroethidium (Molecular Probes, Eugene, OR, USA) was used to investigate the local *in situ* production of ROS. The assay was performed as previously described [27].

Flow Cytometric Determination of Intracellular ROS

The ROS assay kit (S0033; Beyotime Ins. Bio, Jiangsu, China) was used to determine the intracellular ROS generation according to

the manufacturer's instructions. U251 cells were seeded in 6-cell plates and grown for 1–2 days until 70–80% confluence. Then, transfections of the FLAG-CON and the FLAG-JWA in U251 cells were carried out using Lipofectamine 2000 transfection reagent (Invitrogen, Carlsbad, CA, USA) following the manufacturer's protocol. Twelve hours after transfection of FLAG-CON or FLAG-JWA, U251 cells were treated with MPP^+ (50 μM) for 24 h, and then, the cells were incubated with dichloro-dihydrofluorescein diacetate (DCHF-DA) at 37°C (10 μM, 3 mL) for 20 min. Levels of ROS were measured by flow cytometry (EPICS-XL; Beckman Coulter, Miami, FL, USA).

Measurement of Intracellular Glutathione

Commercial kits (Beyotime Ins. Bio) were used to determine the contents of intracellular glutathione (GSH). U251 cells were seeded in 6-cell plates with about 60% confluence. After 12 h transfection of FLAG-CON or FLAG-JWA, the cells were treated with MPP^+ (50 μM) for 24 h. The absorbance was read at 412 nm. Standard curve (0.5, 1.0, 2.0, 5.0, 10.0, and 15.0 μM) of GSH was also established.

Statistical Analysis

All data were presented as mean ± SEM. Statistical comparison was made with Student's *t*-test. $P < 0.05$ was considered statistically significant.

Results

Astrocytic JWA-Deficient Mice are Hypersensitive to MPTP

In the *in vivo* mice model, all the $JWA^{\Delta 2/\Delta 2}$/GFAP-Cre mice died within 6 h, whereas all $JWA^{Loxp/Loxp}$ mice survived after the first treatment of MPTP, indicating that astrocytic JWA expression might be necessary for mice survival in response to acute MPTP challenge. As MPTP is a DA neuron targeting agent, we thus investigated the effects of JWA deficiency in astrocytes on DA neurons.

Astrocytic JWA Deficiency Results in Astrocyte Activation Accompanied by Loss of DA Neurons in Substantia Nigra

Conditional astrocytic JWA KO led to a significant increase in glial fibrillary acidic protein (GFAP)-positive cells in SNc compared with $JWA^{Loxp/Loxp}$ mice ($1.34 \times 10^3 \pm 74.5$ vs. $8.44 \times 10^3 \pm 1.35 \times 10^3$, $P < 0.01$, Figure 2A). Moreover, the number of neurons in SNc of astrocytic JWA conditional KO mice was 30% less than the controls under basic condition by Nissl's staining ($P < 0.001$, Figure 2B). The astrocytic JWA-deficient mice showed a dramatic reduction in TH^+ neuronal number in SNc compared with those in $JWA^{Loxp/Loxp}$ mice ($1.03 \times 10^4 \pm 238$ vs. $6.17 \times 10^3 \pm 392$, $P < 0.001$, Figure 2C). Interestingly, there were no obvious effects on GABA neurons in the striatum and noradrenergic neurons in the mesencephalon between the two mice genotypes (Figure S1B,C). These findings indicated that astrocytic JWA deficiency may result in tissue-specific degeneration of DA neurons in substantia nigra, accompanied with astrocyte activation.

Effect of JWA on Monoamine Neurotransmitters in Mouse Striatum

To examine whether knockout JWA in astrocytes affects DA neurotransmitters in mouse striatum, we measured the levels of dopamine and its metabolites. We found that the dopamine levels were significantly increased in the striatum of $JWA^{\Delta 2/\Delta 2}$/GFAP-Cre mice compared with the control mice (11.1 ± 1.79 nmol/g vs. 22.5 ± 2.23 nmol/g, $P < 0.01$, Figure 3A); whereas the levels of HVA (13.8 ± 0.742 nmol/g vs. 10.6 ± 0.870 nmol/g, $P < 0.05$, Figure 3D) and the ratio of DOPAC/DA (3.28 ± 0.414 vs. 2.02 ± 0.285, $P < 0.05$, Figure 3C) decreased although there was no significant difference in DOPAC (Figure 3B). These data indicated that astrocytic JWA not only affected the generation but also the metabolism of monoamine neurotransmitters in the mouse striatum.

Astrocytic JWA Attenuates Oxidative Damage *In Vivo* and *In Vitro*

Using immunofluorescence assay, we found that the number of TH-positive neurons in SNc of astrocytic JWA conditional KO mice were less than in the controls; however, the levels of either intracellular or extracellular ROS increased (Figure 4A). These findings indicated that absence of JWA in astrocytes promoted ROS production in both glial cells and DA neurons.

To further confirm the above findings, FLAG-JWA was used in human U251 glioma cells. Data showed that JWA overexpression significantly reduced ROS production (the curve shifted to the left) in U251 glioma cells treated with MPP^+ ($3.60 \times 10^4 \pm 572$ vs. $2.87 \times 10^4 \pm 397$, $P < 0.001$, Figure 4B). Moreover, the JWA-overexpressing group had higher GSH levels (298 ± 0.667 pmol/mg vs. 365 ± 7.09 pmol/mg, $P < 0.001$, Figure 4C). These results demonstrated that astrocytic JWA deficiency enhanced oxidative damage in DA neurons *in vivo*, and JWA overexpression enhanced antioxidant capacity while increased MPP^+ induced apoptosis in glioma cells *in vitro*.

JWA Inhibits IKKβ-NF-κB Pathway in Glioma Cells

Considering the important role of NF-κB in ROS production [33], we further determined the NF-κB-related molecular events involved in KO mice with JWA-deficient astrocytes. As a result, the expression of NF-κB-p65 in the nucleus of midbrain tissue was 1.67-fold higher in $JWA^{\Delta 2/\Delta 2}$/GFAP-Cre mice than that of $JWA^{Loxp/Loxp}$ mice ($P < 0.01$, Figure 5A). In the *in vitro* glioma model, JWA overexpression increased NF-κB-p65 2.1-fold ($P < 0.01$) in the cytoplasm and reduced to 70% ($P < 0.001$) of its levels in the nucleus of the U251 cells in response to 50 μM MPP^+ treatment (Figure 5B). These data implied that NF-κB pathway might be involved in regulation of JWA on DA neuron degeneration and astrocyte activation.

To further elucidate the mechanism by which JWA negatively regulates NF-κB-p65, we detected the expression of its upstream

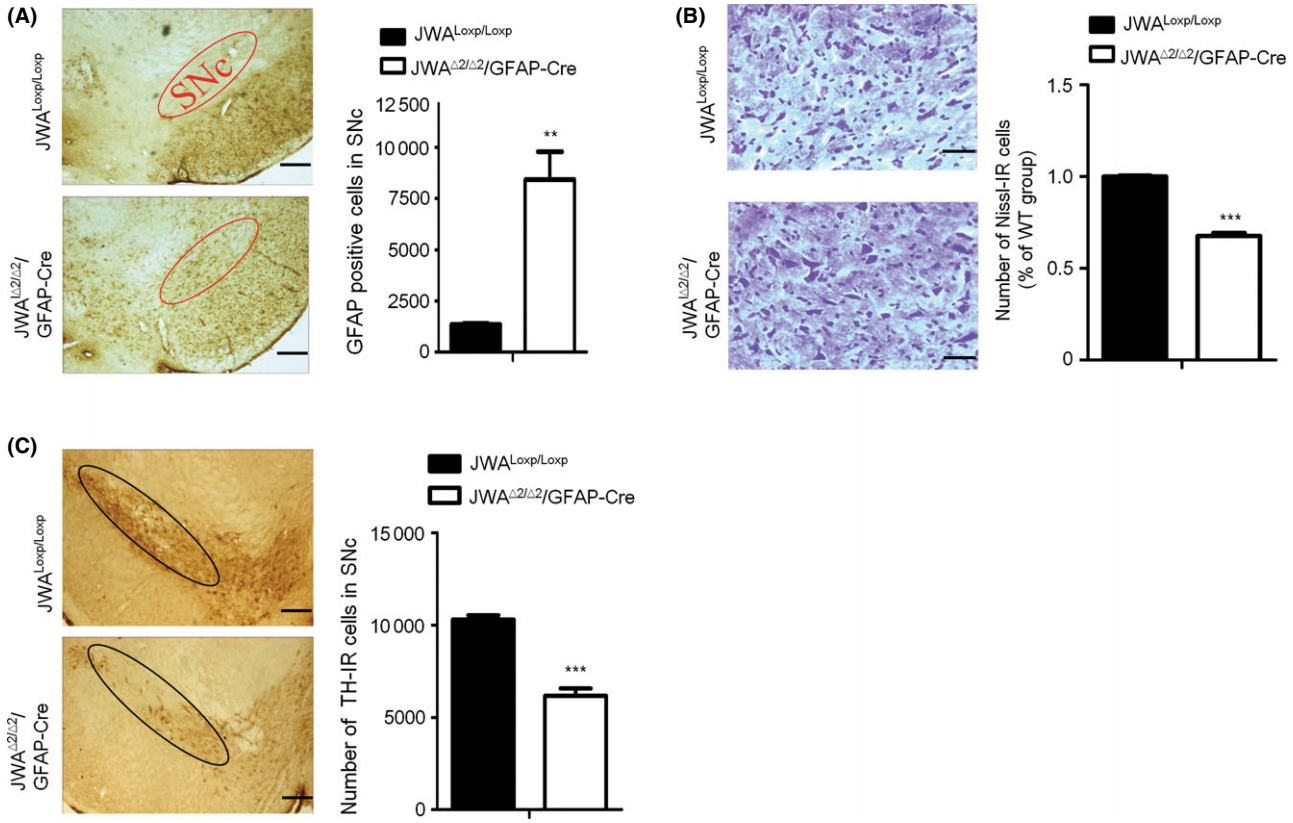

Figure 2 Astrocytic JWA deficiency results in loss of dopaminergic neurons. (**A**) Microphotographs of GFAP-ir cells with ×40 magnification and stereological counts of GFAP-ir cells in mice SNc. Scale bars = 200 μm. (**B**) Microphotographs of Nissl-stained neurons with ×100 magnification and stereological counts of Nissl-stained cells in mice SNc. Scale bars = 100 μm. (**C**) Microphotographs of TH-ir neurons with ×40 magnification and stereological counts of TH-ir cells in mice SNc. Data are expressed as mean ± SD, Scale bars = 200 μm. $^{**}P < 0.01$, $^{***}P < 0.001$, n = 4.

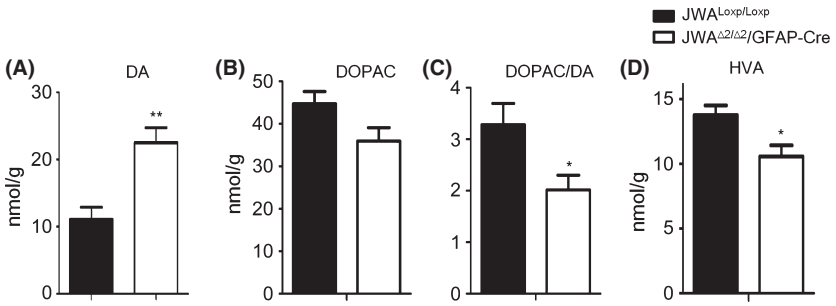

Figure 3 Astrocyte deficiency of JWA induces imbalance of dopamine metabolism in the mouse striatum. The effects of the astrocyte JWA deficiency on the levels of dopaminergic (DA) (**A**), dihydroxyphenylacetic acid (DOPAC) (**B**), DOPAC/DA (**C**), and homovanillic acid (**D**) were determined. Data are expressed as mean ± SD, $^{*}P < 0.05$; $^{**}P < 0.01$, n = 6.

molecule IKKs. We found that the expression of IKKβ was 1.7-fold ($P < 0.05$) in JWA$^{\Delta 2/\Delta 2}$/GFAP-Cre mice, while IκB was 0.5-fold ($P < 0.001$) in the midbrain (Figure 6A). However, no change in IKKα was observed. Consistently, the IκB increased to 1.7-fold, while the IKKβ and p-p65 were approximately 0.6-fold and 0.5-fold in FLAG-JWA cells compared with the parental cells, respectively ($P < 0.001$, Figure 6B). These results indicated that the JWA-IKKβ-NF-κB signaling pathway also might be involved in the pathogenesis of PD.

Discussion

About 50-70% of the DA neurons in PD patients are already lost at the time of clinical diagnosis [34]. Brain homeostasis is critical for the progress of DA neuron degeneration, which is partly maintained by the glial functions [18]. Moreover, substantia nigra in PD patients exhibits increased levels of peroxidated lipids [35], DNA, and proteins [36], as well as decreased levels of GSH [37]. However, the molecular mechanisms responsible for the DA

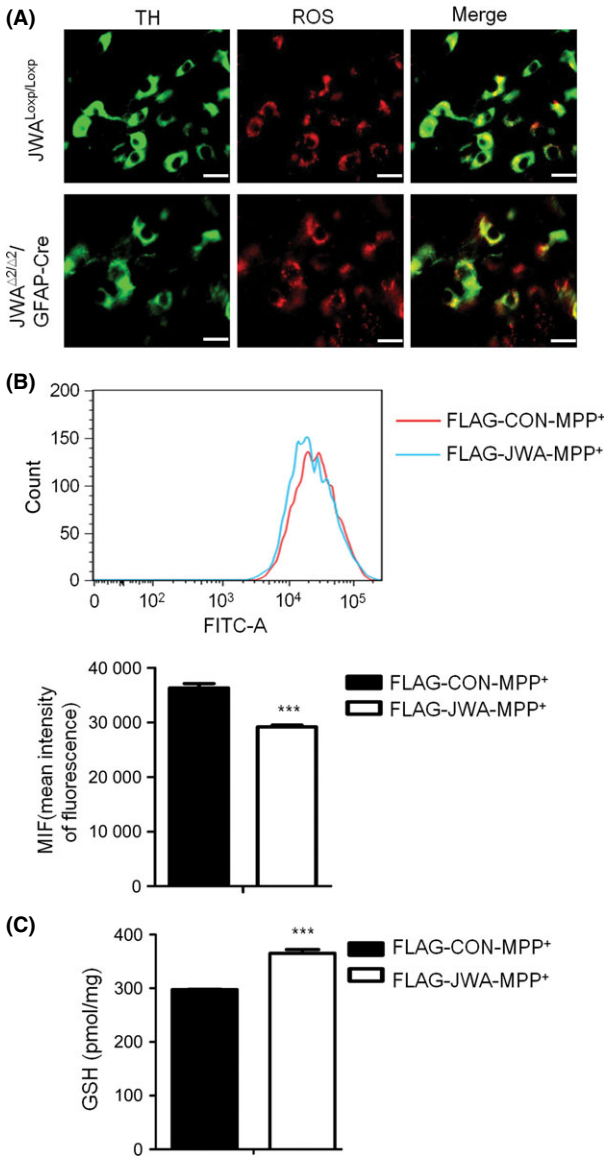

Figure 4 Astrocyte deficiency of JWA induces imbalance of redox *in vivo* and *in vitro*. (**A**) Immunofluorescence staining showed the expression of TH (green) in substantia nigra with reactive oxygen species (ROS) (red). ×200 magnification. Scale bars = 40 μm. (**B**) Flow cytometric determination of ROS in FLAG-JWA-transfected U251 cells. Data are presented as the mean ± SEM, ***$P < 0.001$, n = 3. (**C**) Measurement of contents of intracellular glutathione (GSH) by commercial kits. Data are expressed as mean ± SD, ***$P < 0.001$, n = 3.

degeneration are quite obscure. In this study, we demonstrated, to the best of our knowledge, for the first time that JWA in astrocytes exert an effect on DA neuron degeneration and identified some of the potential mechanisms.

In our conditional astrocytic JWA KO mouse model, we observed a 40% loss of DA neurons with concomitant activation of astrocytes and increased dopamine production compared with the WT mice. Previously, we have shown that the JWA gene responds to environmental stimuli and is a mediator of intracellular antioxidant effects, protecting cells from DNA damage induced by ROS [38]. The mechanism resulting in the loss of DA neurons could be due to the elevation of cytotoxic DA metabolites and ROS, as was shown here, promoting oxidative stress, cytotoxicity, nigrostriatal DA terminal degeneration, and eventually neuronal death [39]. A possible explanation for the increased dopamine levels in striatum could be that the number of striatal TH^+ neurons was significantly greater in parkinsonian monkeys and rodents compared with controls [40–44]. These findings led to the suggestion that midbrain nigral neurons possessed a strong capacity to increase their striatal TH^+ neurons and synaptic neurotransmitter productions to compensate for the loss of DA neurons [45]. Apart from oxidative stress, activation of neuroinflammatory cells, especially astrocytes, with subsequent production of signaling molecules also influences PD genesis [46]. ROS has been shown to challenge intracellular signaling cascades associated with inflammatory response [47] and activate certain transcription factors, notably the NF-κB [48,49]. The present study revealed that astrocytic JWA deficiency induced activation of the NF-κB pathway, suggesting that astrocytic JWA deficiency also can trigger inflammatory response in DA neurons, thus leading to the development of PD in mice by another mechanism. The NF-κB is an active molecule involved in inflammatory response, existing as a cytoplasmic p50/p65 heterodimer which binds to an inhibitory subunit, IκB [50]. Exposure of cells to various pathological stimuli can activate NF-κB and promote the translocation of NF-κB from cytoplasm to nucleus and then regulate expression of the target genes [51]. Here, we showed that the JWA effectively regulated DA neurons via inhibiting NF-κB expression in astrocytes. Deficiency of JWA in astrocytes greatly enhanced NF-κB activation in mesencephalon tissue and U251 cells treated with MPP^+. Suppression of IκB degradation can result in the inhibition of p65 nuclear translocation, and IKKs-IκBα-mediated cytoplasmic accumulation of the NF-κB complex has been regarded as a key mechanism of terminating NF-κB signaling [52,53]. In our study, we showed that JWA can inhibit the activation of NF-κB signaling pathway by the downregulation of IKKβ expression.

Interestingly, a recent association study by Kareus et al. found a significantly elevated risk of melanoma in 7841 PD cases and their relatives [54]. Our recent studies revealed that JWA can functionally inhibit cell adhesion, invasion, and metastasis of melanoma cells via suppressing integrin αVβ3 signaling [55]. Taken together, we propose that congenital or acquired expression deficiency of environmental responsive genes like JWA could be a common molecular feature of PD and melanoma. The deficiency or loss of JWA may result in dysregulation or imbalance of redox signal network that triggers the activation of NF-κB and signaling pathways associated with integrin. Finally, we showed that JWA deficiency in astrocytes can lead to DA neuronal damage directly without MPTP exposure and that conditional astrocyte JWA KO mice do not tolerate the toxicity of MPTP, unlike many genes or drugs that could exert effects on DA degeneration indirectly in response to MPTP treatment [19,27]. Thus, conditional KO of JWA in astrocytes could possibly be used to establish a natural model of PD in mice. Our *in vitro* results obtained with U251 human

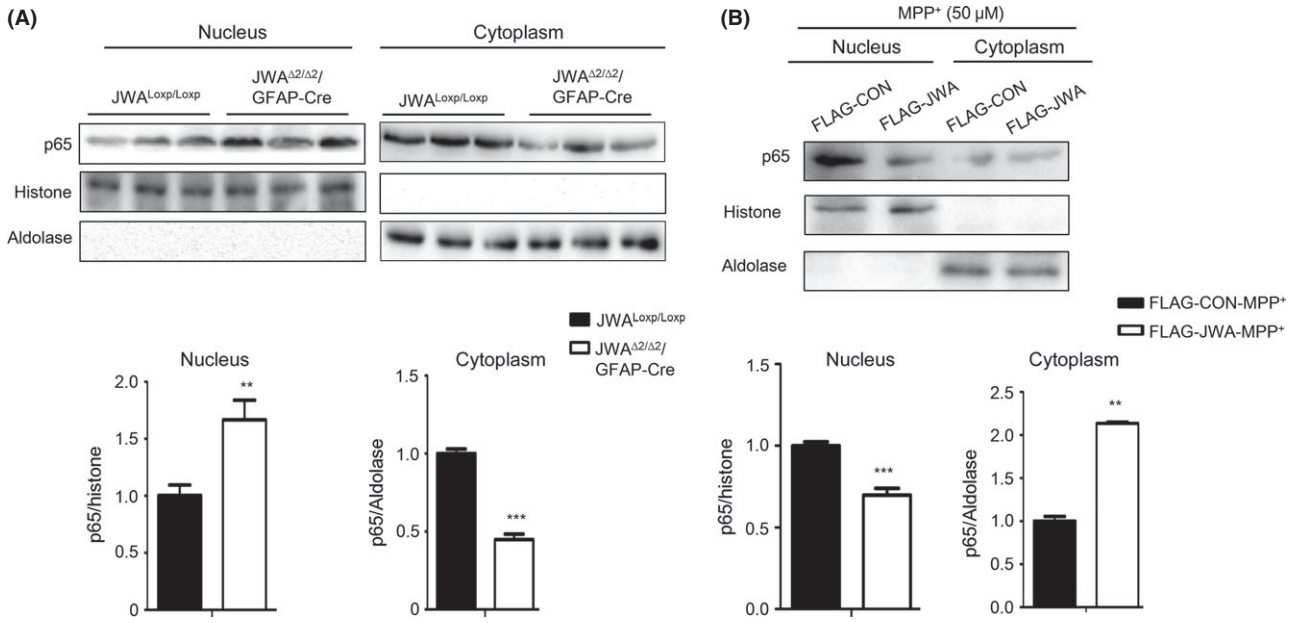

Figure 5 Deficiency of JWA promotes nuclear factor (NF)-κB-p65 translocation. (**A**) The protein expression of p65 in nucleus and cytoplasm in mesencephalon of each group of mice were determined by Western blot. Histone H1 and aldolase were used as the nuclear and cytoplasmic loading controls, respectively. n = 4. (**B**) The protein expression of p65 in nucleus and cytoplasm after FLAG-JWA transfection during 1-methyl-4-phenylpyridinium (MPP^+) treatment in U251 cells. Histone H1 and aldolase were used as nuclear and cytoplasmic loading controls, respectively. Data are expressed as mean ± SD, $^{**}P < 0.01$; $^{***}P < 0.001$.

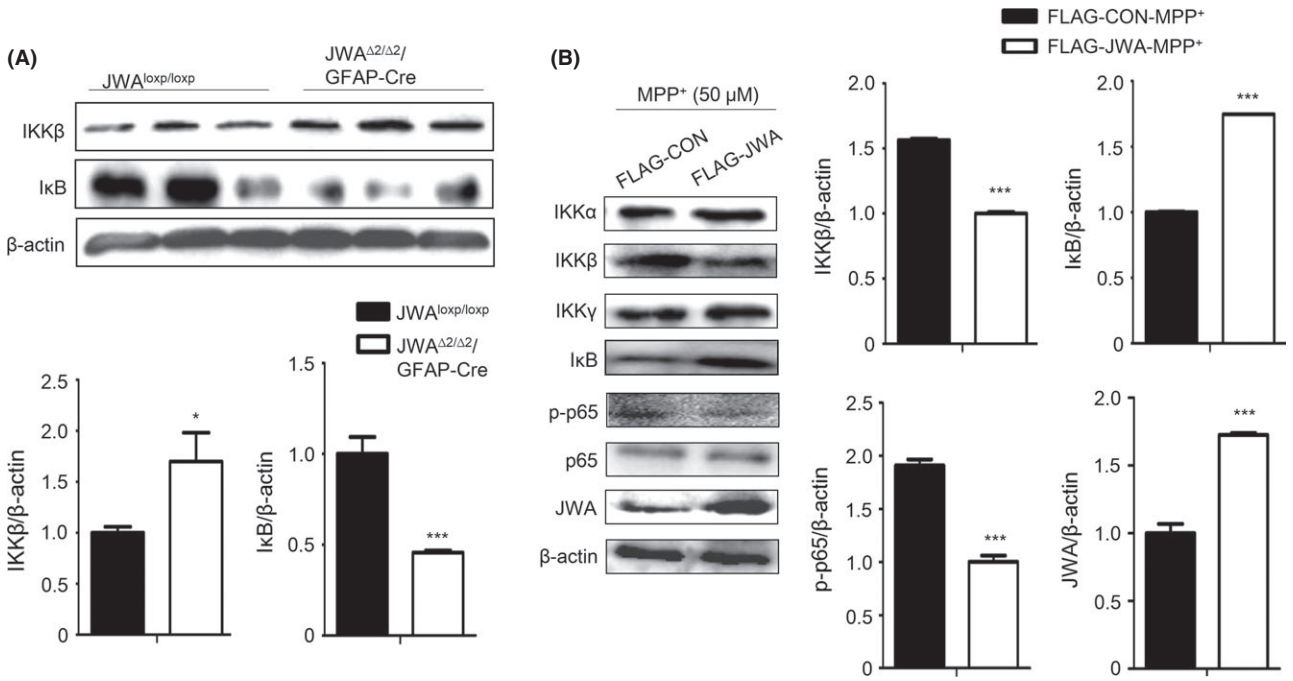

Figure 6 Deficiency of JWA-activated IKKβ-IκB-nuclear factor (NF)-κB pathway. (**A**) The protein expression of IKKβ and IκB in mesencephalon of each group of mice. Data are expressed as mean ± SD, $^{*}P < 0.05$; $^{***}P < 0.001$, n = 3. (**B**) The expression of NF-κB pathway after FLAG-JWA transfection during 1-methyl-4-phenylpyridinium (MPP^+) treatment in U251 cells. Data are expressed as mean ± SD, $^{***}P < 0.001$.

cell line are generally consistent with those observed *in vivo* or *ex vivo* in mice. The clinical relevance of these data is underscored by the use of a human astrocytic cell line (even derived from glioblastoma), although similar experiments with primary mice astrocytes would further consolidate the significance of molecular and cellular mechanisms discussed herein.

In summary, our study provided evidence that astrocytic JWA expression protects DA neurons from degeneration and plays an important role in neuroprotection via inhibition of ROS and NF-κB activation. These findings indicate that JWA might be a novel potential therapeutic target for human PD.

Acknowledgments

We thank Dr. Oluf Dimitri Røe of the Norwegian University of Science and Technology (NTNU) for helpful discussions and language revision. This study was supported in part by the Natural Science Foundation of China (Grant Numbers: 30930080, 91229125).

Conflict of Interest

The authors declare no conflict of interest.

References

1. Teismann P, Tieu K, Choi DK, et al. Cyclooxygenase-2 is instrumental in Parkinson's disease neurodegeneration. *Proc Natl Acad Sci USA* 2003;**100**:5473–5478.
2. Moore DJ, West AB, Dawson VL, Dawson TM. Molecular pathophysiology of Parkinson's disease. *Annu Rev Neurosci* 2005;**28**:57–87.
3. Dauer W, Przedborski S. Parkinson's disease: Mechanisms and models. *Neuron* 2003;**39**:889–909.
4. Jackson-Lewis V, Blesa J, Przedborski S. Animal models of Parkinson's disease. *Parkinsonism Relat Disord* 2012;**18** (Suppl 1):S183–S185.
5. Dawson TM, Dawson VL. Molecular pathways of neurodegeneration in Parkinson's disease. *Science* 2003;**302**:819–822.
6. Kincses ZT, Vecsei L. Pharmacological therapy in Parkinson's disease: Focus on neuroprotection. *CNS Neurosci Ther* 2011;**17**:345–367.
7. Yoo MS, Chun HS, Son JJ, et al. Oxidative stress regulated genes in nigral dopaminergic neuronal cells: Correlation with the known pathology in Parkinson's disease. *Brain Res Mol Brain Res* 2003;**110**:76–84.
8. Chan P, DeLanney LE, Irwin I, Langston JW, Di Monte D. Rapid ATP loss caused by 1- methyl-4-phenyl-1,2,3,6-tetrahydropyridine in mouse brain. *J Neurochem* 1991;**57**: 348–351.
9. Nicotra A, Parvez S. Apoptotic molecules and MPTP-induced cell death. *Neurotoxicol Teratol* 2002;**24**:599–605.
10. Xu H, Jiang H, Wang J, Xie J. Rg1 protects the MPP^+-treated MES23.5 cells via attenuating DMT1 up-regulation and cellular iron uptake. *Neuropharmacology* 2010;**58**:488–494.
11. Hayden MS, West AP, Ghosh S. NF-kappaB and the immune response. *Oncogene* 2006;**25**:6758–6780.
12. Tilstra JS, Robinson AR, Wang J, et al. NF-kappaB inhibition delays DNA damage-induced senescence and aging in mice. *J Clin Invest* 2012;**122**:2601–2612.
13. Sidoryk-Wegrzynowicz M, Wegrzynowicz M, Lee E, Bowman AB, Aschner M. Role of astrocytes in brain function and disease. *Toxicol Pathol* 2011;**39**: 115–123.
14. Pekny M, Nilsson M. Astrocyte activation and reactive gliosis. *Glia* 2005;**50**:427–434.
15. Maragakis NJ, Rothstein JD. Glutamate transporters in neurologic disease. *Arch Neurol* 2001;**58**:365–370.
16. Walz W. Role of astrocytes in the clearance of excess extracellular potassium. *Neurochem Int* 2000;**36**:291–300.
17. Belanger M, Allaman I, Magistretti PJ. Brain energy metabolism: Focus on astrocyte-neuron metabolic cooperation. *Cell Metab* 2011;**14**:724–738.
18. Rappold PM, Tieu K. Astrocytes and therapeutics for Parkinson's disease. *Neurotherapeutics* 2010;**7**:413–423.
19. Lu M, Fan Y, Tang M, Qian X, Ding J, Hu G. Potentiation of D-serine involves degeneration of dopaminergic neurons in MPTP/p mouse model of Parkinson's disease. *CNS Neurosci Ther* 2011;**17**:796–798.
20. Chen H, Bai J, Ye J, et al. JWA as a functional molecule to regulate cancer cells migration via MAPK cascades and F-actin cytoskeleton. *Cell Signal* 2007;**19**:1315–1327.
21. Huang S, Shen Q, Mao WG, et al. JWA, a novel signaling molecule, involved in all-trans retinoic acid induced differentiation of HL-60 cells. *J Biomed Sci* 2006;**13**:357–371.
22. Huang S, Shen Q, Mao WG, et al. JWA, a novel signaling molecule, involved in the induction of differentiation of human myeloid leukemia cells. *Biochem Biophys Res Commun* 2006;**341**:440–450.
23. Wang S, Gong Z, Chen R, et al. JWA regulates XRCC1 and functions as a novel base excision repair protein in oxidative-stress-induced DNA single-strand breaks. *Nucleic Acids Res* 2009;**37**:1936–1950.
24. Chen R, Qiu W, Liu Z, et al. Identification of JWA as a novel functional gene responsive to environmental oxidative stress induced by benzo[a]pyrene and hydrogen peroxide. *Free Radic Biol Med* 2007;**42**:1704–1714.
25. Gong Z, Shi Y, Zhu Z, et al. JWA deficiency suppresses dimethylbenz[a]anthracene-phorbol ester induced skin papillomas via inactivation of MAPK pathway in mice. *PLoS One* 2012;**7**:e34154.
26. Shao W, Zhang SZ, Tang M, et al. Suppression of neuroinflammation by astrocytic dopamine D2 receptors via alphaB-crystallin. *Nature* 2013;**494**:90–94.
27. Lu M, Zhao FF, Tang JJ, et al. The neuroprotection of hydrogen sulfide against MPTP-induced dopaminergic neuron degeneration involves uncoupling protein 2 rather than ATP-sensitive potassium channels. *Antioxid Redox Signal* 2012;**17**:849–859.
28. Xie LL, Sun XL, Fan Y, Kong H, Ding JH, Hu G. Aquaporin 4 knockout resists negative regulation of neural cell proliferation by cocaine in mouse hippocampus. *Int J Neuropsychopharmacol* 2009;**12**:843–850.
29. Kilic E, ElAli A, Kilic U, et al. Role of Nogo-A in neuronal survival in the reperfused ischemic brain. *J Cereb Blood Flow Metab* 2010;**30**:969–984.
30. Yang W, Wu Q, Yuan C, et al. Aquaporin-4 mediates astrocyte response to beta-amyloid. *Mol Cell Neurosci* 2012;**49**:406–414.
31. Shen L, Xu W, Li A, Ye J, Zhou J. JWA enhances As(2)O(3)-induced tubulin polymerization and apoptosis via p38 in HeLa and MCF-7 cells. *Apoptosis* 2011;**16**:1177–1193.
32. Wang S, Wu X, Zhang J, et al. CHIP functions as a novel suppressor of tumour angiogenesis with prognostic significance in human gastric cancer. *Gut* 2013;**62**:496–508.
33. Lee HJ, Kim SH, Kim KW, et al. Antiapoptotic role of NF-kappaB in the auto-oxidized dopamine-induced apoptosis of PC12 cells. *J Neurochem* 2001;**76**:602–609.
34. Morrish PK, Rakshi JS, Bailey DL, Sawle GV, Brooks DJ. Measuring the rate of progression and estimating the preclinical period of Parkinson's disease with [18F]dopa PET. *J Neurol Neurosurg Psychiatry* 1998;**64**:314–319.
35. Bosco DA, Fowler DM, Zhang Q, et al. Elevated levels of oxidized cholesterol metabolites in Lewy body disease brains accelerate alpha-synuclein fibrilization. *Nat Chem Biol* 2006;**2**:249–253.
36. Nakabeppu Y, Tsuchimoto D, Yamaguchi H, Sakumi K. Oxidative damage in nucleic acids and Parkinson's disease. *J Neurosci Res* 2007;**85**:919–934.
37. Zeevalk GD, Razmpour R, Bernard LP. Glutathione and Parkinson's disease: Is this the elephant in the room? *Biomed Pharmacother* 2008;**62**:236–249.
38. Chen R, Li A, Zhu T, et al. JWA – A novel environmental-responsive gene, involved in estrogen receptor-associated signal pathway in MCF-7 and MDA-MB-231 breast carcinoma cells. *J Toxicol Environ Health A* 2005;**68**:445–456.
39. Lotharius J, Brundin P. Impaired dopamine storage resulting from alpha-synuclein mutations may contribute to the pathogenesis of Parkinson's disease. *Hum Mol Genet* 2002;**11**:2395–2407.
40. Tashiro Y, Sugimoto T, Hattori T, et al. Tyrosine hydroxylase-like immunoreactive neurons in the striatum of the rat. *Neurosci Lett* 1989;**97**:6–10.
41. Betarbet R, Turner R, Chockkan V, et al. Dopaminergic neurons intrinsic to the primate striatum. *J Neurosci* 1997;**17**:6761–6768.
42. Meredith GE, Farrell T, Kellaghan P, Tan Y, Zahm DS, Totterdell S. Immunocytochemical characterization of catecholaminergic neurons in the rat striatum following dopamine-depleting lesions. *Eur J Neurosci* 1999;**11**:3585–3596.
43. Mao L, Lau YS, Petroske E, Wang JQ. Profound astrogenesis in the striatum of adult mice following nigrostriatal dopaminergic lesion by repeated MPTP administration. *Brain Res Dev Brain Res* 2001;**131**: 57–65.
44. Mazloom M, Smith Y. Synaptic microcircuitry of tyrosine hydroxylase-containing neurons and terminals in the striatum of 1-methyl-4-phenyl-1,2,3,6-tetrahydropyridine-treated monkeys. *J Comp Neurol* 2006;**495**:453–469.
45. Huot P, Levesque M, Parent A. The fate of striatal dopaminergic neurons in Parkinson's disease and Huntington's chorea. *Brain* 2007;**130**:222–232.
46. Marchetti B, Abbracchio MP. To be or not to be (inflamed)–is that the question in anti-inflammatory drug therapy of neurodegenerative disorders? *Trends Pharmacol Sci* 2005;**26**:517–525.
47. Droge W. Free radicals in the physiological control of cell function. *Physiol Rev* 2002;**82**:47–95.
48. Kim JC, Lee YH, Yu MK, et al. Anti-inflammatory mechanism of PPARgamma on LPS-induced pulp cells: Role of the ROS removal activity. *Arch Oral Biol* 2012;**57**:392–400.
49. Zhao H, Wang SL, Qian L, et al. Diammonium glycyrrhizinate attenuates Abeta(1-42) -induced neuroinflammation and regulates MAPK and NF-kappaB pathways *in vitro* and *in vivo*. *CNS Neurosci Ther* 2013;**19**:117–124.
50. Lenardo MJ, Baltimore D. NF-kappa B: A pleiotropic mediator of inducible and tissue-specific gene control. *Cell* 1989;**58**:227–229.
51. Pahl HL, Baeuerle PA. The ER-overload response: Activation of NF-kappa B. *Trends Biochem Sci* 1997;**22**:63–67.

52. Arenzana-Seisdedos F, Thompson J, Rodriguez MS, Bachelerie F, Thomas D, Hay RT. Inducible nuclear expression of newly synthesized I kappa B alpha negatively regulates DNA-binding and transcriptional activities of NF-kappa B. *Mol Cell Biol* 1995;**15**:2689–2696.
53. Arenzana-Seisdedos F, Turpin P, Rodriguez M, et al. Nuclear localization of I kappa B alpha promotes active transport of NF-kappa B from the nucleus to the cytoplasm. *J Cell Sci* 1997;**110**(Pt 3):369–378.
54. Kareus SA, Figueroa KP, Cannon-Albright LA, Pulst SM. Shared predispositions of parkinsonism and cancer: A population-based pedigree-linked study. *Arch Neurol* 2012;**69**:1572–1577.
55. Bai J, Zhang J, Wu J, et al. JWA regulates melanoma metastasis by integrin alphaVbeta3 signaling. *Oncogene* 2010;**29**:1227–1237.

Supporting Information

The following supplementary material is available for this article:

Figure S1. Astrocytes deficiency of JWA had no obvious effects on JWA expression level in DA neurons and had no effects on noradrenergic neurons and GABA neurons.

